crystals

MDPI

Article

Crystal Growth of RuS_2 Using a Chemical Vapor Transport Technique and Its Properties

Refka Sai [1,2,*], Ouri Gorochov [3], Eman A. Alghamdi [4] and Hatem Ezzaouia [1]

[1] Laboratory of Semiconductors, Nanostructures and Advanced Technologies, Borj Cedria Science and Technology Park, BP 95, Hammam-Lif 2050, Tunisia; ezzaouia.hatem@inrst.rnrt.tn
[2] Departement de Physique, Faculté des Sciences de Bizerte, Université de Carthage, Tunis 7021, Tunisia
[3] Groupe d'Etude de la Matière Condensée, CNRS-Université de Versailles St-Quentin 1, Place A, Briand, CEDEX, F-92195 Meudon, France; gorochov@cnrs-bellevue.fr
[4] Department of Physics and Astronomy, King Saud University, Riyadh 11451, Saudi Arabia; ialghamidi@ksu.edu.sa
* Correspondence: refka.sai@fsb.ucar.tn

Abstract: In this work, we study the effect of increasing temperature on the structure parameters (lattice, sulfur–sulfur distance, and ruthenium–sulfur distance) and the energy gap of RuS_2. However, it was very challenging to obtain a sample of RuS_2 due to many factors, some of which are discussed in the introduction. To prepare the crystal growth of RuS_2, we have used the chemical vapor transport technique. The crystals obtained show a pyrite structure, of which we studied its crystallographic structure, including the structure of crystals in surface (100). The sample was then characterized by X-ray diffraction and by microprobe analysis. We determine the relationship between the energy gap and the sulfur–sulfur distance. We analyzed the S-S bond compared with the S_2 molecule.

Keywords: pyrite RuS_2; crystal growth; band gap; chemical vapor transport

Citation: Sai, R.; Gorochov, O.; Alghamdi, E.A.; Ezzaouia, H. Crystal Growth of RuS_2 Using a Chemical Vapor Transport Technique and Its Properties. *Crystals* **2022**, *12*, 994. https://doi.org/10.3390/cryst12070994

Academic Editors: Drialys Cardenas-Morcoso, Hung-Pin Hsu and Franziska Simone Hegner

Received: 13 June 2022
Accepted: 11 July 2022
Published: 17 July 2022

1. Introduction

The aim of this work is the study of the effect of the sulfur–sulfur distance on the electronic and optical properties of the RuS_2 pyrite. Over the past few years much attention has been given to the study of sulfur-containing compounds. This tendency is due to the increasing environmental issues, as well as academic interests [1]. Ruthenium Sulfide, RuS_2 is one of the interesting sulfur compounds from both fundamental and technological points of view. It is one of the semiconducting transition-metal dichalcogenide (TMDC) materials, with a reported band gap of 1.8 eV [2] and has a pyrite structure [3]. Ruthenium Sulfide, RuS_2 has several possible uses, including its use as a catalyst [4] and as a photoelectrode [5–8]. However, it is difficult to obtain the crystalline RuS_2 due to several facts, for instance we can obtain RuS_2 only at temperatures greater than 1000 °C. Therefore, obtaining its crystalline structure at low temperatures is practically impossible. Moreover, the physical vapor transport method is difficult to use because the vapor pressure of RuS_2 is very low, at temperatures between 800 and 1050 °C.

Our work is structured as follows. First, we provide a detailed description of the experimental procedure used to obtain RuS_2 by the chemical vapor transport technique. Next, we provide a brief description of the techniques and tools used to analyze the obtained sample, such as X-ray diffraction and microprobe analysis. In addition, we provide a detailed analysis of our findings; that is, the influence of increasing temperature on the stoichiometry shift of sulfur, *S* and how the different values of the energy gap helped us to understand and analyze the effect of other parameters, such us temperature, sulfur–sulfur distance, and ruthenium–sulfur distance on the energy gap. Moreover, and as one of our results demonstrates, we show the correlation between the sulfur–sulfur bond and energy gap.

The study of the surface is an important key toward understanding the effect of distribution of sulfur nanoparticles on the value of band gap. Finally, to further understand the interaction between the RuS_2 nanoparticles and surface bonding, we clarified the electronic processes that relate to the bonding in the surface of RuS_2 nanoparticles.

2. Experimental Section

In this work we carry out the chemical vapor transport (CVT) growth in a closed quartz ampule. The phase vapor transport is carried out using silica ampules containing RuS_2 powder and a very low percentage of sulfur. The ampule is 200 mm in length and 25 mm in diameter. The ampule is sealed under chlorine atmosphere (100 mm of Hg). We started crystallization of RuS_2; we used lCl_3 and S_2Cl_2 as transport agents. After, we introduced a small quantity of the oxygen form RuO_2. In the end, the quantity of chlorine and RuO_2 determined 2 atmospheres of $RuOCl_2$ in total at 900°C. The $RuOCl_2$ was then annealed in a dynamical vacuum of 2 atmospheric pressures at a temperature of 900 °C. The crystal growth took place in a graphite-covered quartz ampule.

The mixture $RuS_2 + RuO_2 + Cl_2$ was used as the chemical agent to transport the material from the warm to the cool zone. The temperature of the source materials was between 900 °C and 1025 °C. The crystallization took place in the ampule where the temperature was reduced by 50 °C after each crystallization. The growth region was situated in a hot zone, 925–1050 °C. The duration of transport was between 7 and 15 days. Mono-crystalline RuS_2 was formed in the cool zone of the ampule. By this method, we obtained a polycrystalline structure that consists of mono-crystal grains where the dimensions can decrease from 4 mm × 4 mm × 4 mm to 0.5 mm × 0.2 mm × 0.2 mm. The color of the obtained crystal varies based on the temperature from dark gray to shiny light gray; our result is listed in Table 1.

Table 1. The change of the color of grain crystal. This change is associated with a percentage of concentration of sulfur and the temperature. Additionally, the color of crystals related to the dimension of the grain. However, we succeeded in obtaining RuS_2 by the chemical vapor transport technique.

Sample	Temperature	(%) of extra Sulfure in RuS_2	Color of Monocristal	Size (mm)
CS_1	1050 °C	1	White and dull	4 × 4 × 4
CS_2	1050 °C	2	Dull gray	4 × 4 × 3
CS_3	1025 °C	1	Dull gray	4 × 4 × 3
CS_4	1025 °C	2	Dull gray	4 × 3.5 × 3
CS_5	1000 °C	1	Dull gray	3.5 × 3.5 × 3
CS_6	1000 °C	2	Light gray	3.5 × 3 × 3
CS_7	950 °C	1	Shiny gray	2.5 × 2 × 2
CS_8	950 °C	2	Shiny gray	2 × 2 × 1.5
CS_9	900 °C	1	Very Shiny gray	0.5 × 0.2 × 0.2

We have noticed that the better quality of RuS_2 was obtained at the lowest temperature, which makes this technique of chemical vapor transport very interesting. The importance of this technique is the ability to lower the crystallization temperature of the most refractory materials.

Given the fact that the thermal stability of RuS_2 (Pdissociation = 5 mbar at T = 1100 °C) which is a high temperature. It is impossible to transport halides between 800 and 850 °C and that is since the vapor pressure of ruthenium containing species is low. So far, the CVT of RuS_2 has not been a successful growth method; for example, see [9]. However, for us we succeed in forming RuO_xCl_y when it is transported at a low temperature, and that is due the fact that we used oxygen from RuO_2. Figure 1, shows the growth of monocrystal of RuS_2 by CVT.

Figure 1. Growth of monocrystal of RuS_2 by CVT.

3. Analysis

Several different single crystals of RuS_2 grown by the above technique have been analyzed by microprobe and X-ray diffraction.

3.1. Analysis by Microprobe

We used microprobe casting (camera MS 46–CNRS de Bellevue), which provides a specific chemical analysis using an accelerated and focused electron beam on the sample ($\Phi < 1$ μm at the surface of the sample). Under the effect of electron bombardment, the single crystal produces an X emission of lines characteristic of the elements present. The main reason for using microprobe casting is to observe the influence of both the chemical vapor transport method and the temperature increase in the stoichiometry shift of the sulfur (S) rich atmosphere. As expected, a significant influence on the obtained concentration of RuS_2 was observed. In Table 2, we can see the heavy influence of temperature on the stoichiometry shift of sulfur, S. When the temperature increases, we do not obtain exactly RuS_2, instead the quantity of sulfide slightly decreases, and therefore obtaining a sample of RuS_2 is challenging, as mentioned in the introduction.

Table 2. Analysis of crystals formed by CVT technique.

Sample	Temperature	Excess of S in for RuS_2	Analysis of Composition at Microprobe	Amount of Precipitate O_2
CS1	1050 °C	1	$RuS_{1.90}$	0.005
CS2	1050 °C	2	$RuS_{1.92}$	0.005
CS4	1025 °C	2	$RuS_{1.94}$	-
CS5	1000 °C	1	$RuS_{1.95}$	-
CS7	950 °C	1	$RuS_{1.96}$	-
CS9	900 °C	1	$RuS_{1.97}$	-

In these preliminary results we have not observed the micro-weight of oxygen or anything chloric. It has been observed that as the temperature increases, sulfur concentration decreases, and the material becomes more nonstoichiometric: see Figure 2.

As can be seen, where the temperature increases, the stoichiometry shift of sulfur decreases.

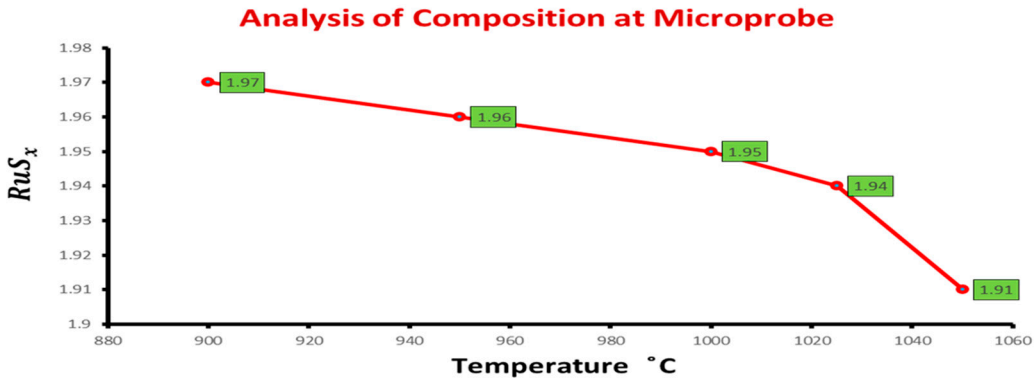

Figure 2. The effect of temperature on sulfur concentration.

3.2. Analysis by X-ray

Powder X-ray diffraction measurements were made on crushed crystals using a Philips diffractometer with CuKα radiation. Cell parameters were calculated, with the aid of a computer, using a least-squares refinement program. Selected crystals were also examined by microprobe casting. Powder X-ray diffraction patterns showed the cubic, with lattice parameters close to the literature value of 5.609–5.635 [10], where RuS_2 crystallizes as laurite in a pyrite type structure, in which disulfide ions are octahedrally coordinated to the Ru metal ion; having the space group symmetry T_h^6 (Pa3), the lattice parameters are the same as in ASTM file. The calculated experimental values for constant lattice a, parameter of structure ν, sulfur–sulfur distance d_{s-s} and Ruthenium–sulfur distance d_{Ru-s} are listed in Table 3.

Table 3. Parameters of cells.

Sample	Temperature	S_2 (%)	a(Å)	ν	$d_{S\text{-}S} \in$ Å	$d_{Ru\text{-}s} \in$ Å
CS1	1050 °C	1	5635	0.1085	2.118	2.369
CS3	1025 °C	1	5630	0.1072	2.097	2.370
CS5	1000 °C	1	5624	0.1075	2.094	2.367
CS6	1000 °C	2	5617	0.1055	2.052	2.369
CS7	950 °C	1	5611	0.105	2.041	2.368
CS9	900 °C	1	5.609	0.101	1.990	2.373

In terms of bond distances, we can see that the $Ru-S$ bond decreases from 2.373 back to 2.367 . The S_2 pair is a weakening of the $S-S$ bond, as the calculated bond length increases when the temperature increases from 900 °C to 1050 °C. To recover the well-known bond character within the S_2 molecules. The $S-S$ bond increases from 1.990 Å to 2.118 Å. The effect of the temperature to bonding in the RuS_2. is shown in Figures 3 and 4, which parameters of structure ν define the atomic position of sulfur. Both the $S-S$ and $Ru-S$ bonds increase with temperature. Thus, they conclude the influence of temperature to parameter structure ν, it is presented in Figure 4 ν increases when temperature increases. The precise bond for the structure (Ru-S and S-S distances) comes from the balance between the temperature and the method to prepare RuS_2. Hence, we deduce that the structure of RuS_2. depends heavily on the temperature.

Next, by using the results of our experimental work we provide more details about the relationship between the structure of RuS_2 and the temperature, along with the effect of the temperature and the $S-S$ bond on the gap energy.

We have determined that there are different values of the energy gap of RuS_2. These values are listed in Table 4 below. In Figure 5, we plotted $(\alpha h\nu)^{\frac{1}{2}}$ versus $h\nu$ photon energy.

From this graph we conclude that pyrite RuS_2 is a semiconductor, has an indirect band gap, and different values of band gap.

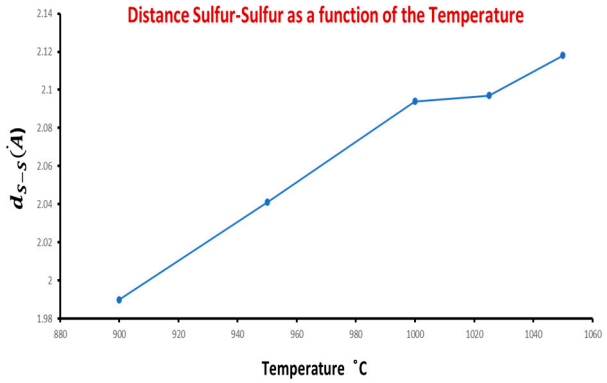

Figure 3. Sulfur–sulfur distance versus temperature.

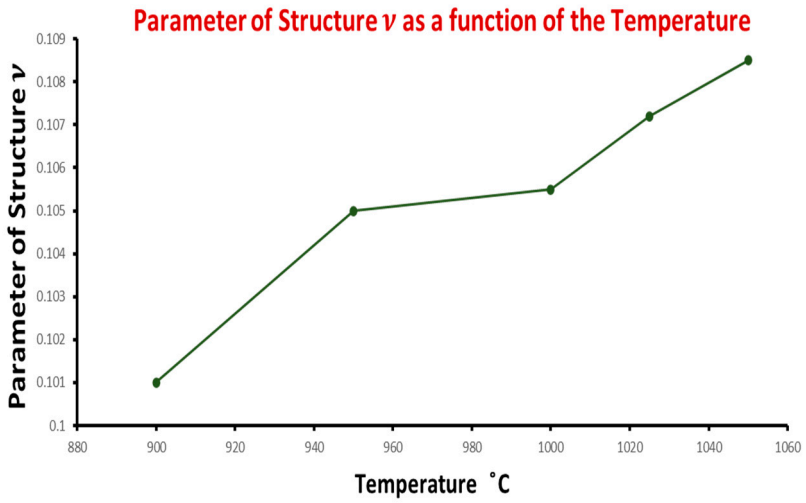

Figure 4. Parameter of structure ν versus temperature.

Table 4. Exprimental parameters.

Sample	Temperature	(%)S	a in Å	Concentration of RuS_x	Eg Experimental (eV)
CS1	1050 °C	1	5.635	$RuS_{1.90}$	1.25
CS3	1025 °C	1	5.630	$RuS_{1.92}$	1.29
CS5	1000 °C	1	5.624	$RuS_{1.95}$	1.36
CS6	1000 °C	2	5.617	$RuS_{1.96}$	1.38
CS7	950 °C	1	5.611	$RuS_{1.96}$	1.42
CS9	900 °C	1	5.609	$RuS_{1.97}$	1.68

The results show a clear and strong dependency of the energy gap on temperature (Figure 6a) and show an extraordinary decrease in the energy gap when the crystallization of the samples is carried out at high temperatures. It is also clear that when the excess of sulfur increases, the energy gap decreases (Figure 6b). However, we have determined the relationship between the growth parameters (temperature, lattice, and distance) and the energy gap. Table 5 shows that the S-S bond is in good agreement with crystallographic data and the elongation of the S-S bond compared with the S_2 molecule. As the resulting energy gap decreases (from 1.68 to 1.25 eV), the sulfur–sulfur distance increases (from

1.990 to 2.118 Å). This clearly shows that the energy gap is strongly dependent on the S-S distance. However, all founded values of the energy gap have the same type of S-S bond in RuS_2. Moreover, the interesting property of RuS_2 is that, regardless of the change of the value of energy gap, it keeps pairs of sulfur S_2 and not an individual S atom. In our study, the sample CS9 has smallest dimension, it was prepared at the lowest temperature of 900 °C and it has the highest band gap 1.68 eV, which shows that the morphology of crystal RuS_2 strongly depends on the band gap and temperature, especially the distribution of sulfur, similar to the work carried out by Aqueel et al. in [11] where they showed the temperature effect on the morphology of $CuCo_2S_4$.

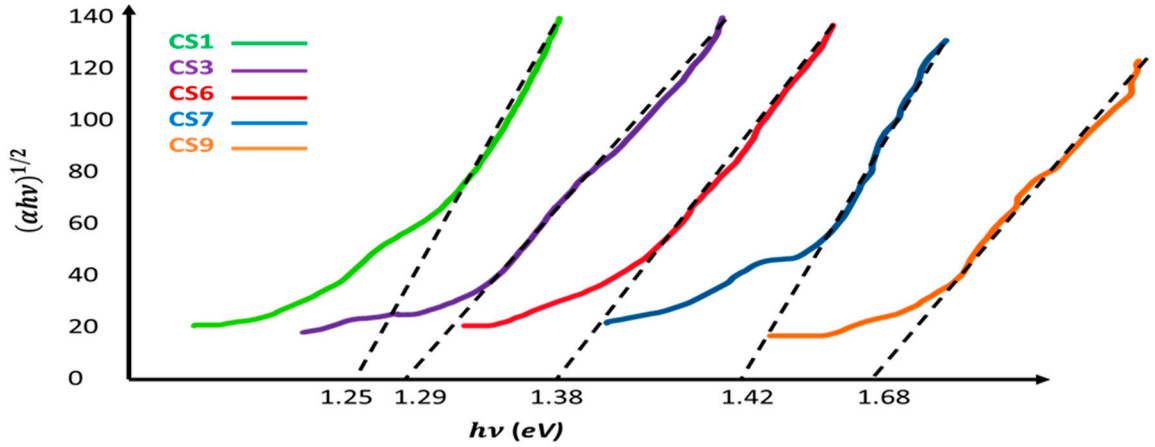

Figure 5. $(\alpha hv)^{\frac{1}{2}}$ versus hv.

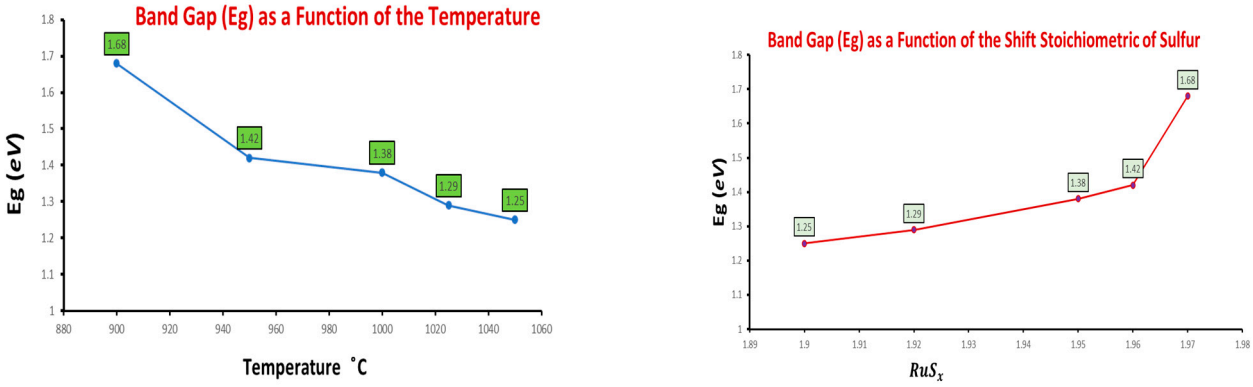

(**a**) (**b**)

Figure 6. (**a**) Band gap versus temperature, (**b**) band gap versus stoichiometric shift of Sulfur.

Table 5. Exprimental crystals paramaters.

Samples	$d_{S\text{-}S}(\AA)$	Eg (eV)	Temperature (°C)
CS1	2.118	1.25	1050
CS3	2.097	1.29	1025
CS5	2.094	1.36	1000
CS7	2.041	1.42	950
CS9	1.990	1.68	900

The pyrite structure of RuS_2 is schematically shown in Figure 7a,b. From the two figures, we can see that the pyrite RuS_2 presents as a face-centered cube of Ru. Figure 7c

presents S_2 molecules, it is clear there are molecules similar to RuS_2, which we have at the cube center, and in the middle of the cube edges (in RuS_2 molecules) S_2 molecules are located. However, RuS_2 appears as S_2 pairs coordinating a metal center. Each Ru atom is in an octahedral arrangement surrounded by six S_2 molecules. Moreover, only one S of each pair is bonded to the Ru atom and the bonds from the metal atom are arranged in a distorted octahedron. Each S atom has three Ru neighbors, and a S_2 pair has six metal neighbors in a pseudo-octahedral coordination. Figure 7d shows that RuS_2 has only the S-S bond type in this structure. Even that can show significant variation of energy gap values of RuS_2, and it is therefore important to understand the S-S bond in the RuS_2 and how it affects the energy gap. This is why it is important to study the surface (100) of pyrite RuS_2. The Figure 8 results show the structure of surface (100) and surface (110). It proved that small nanoparticles of sulfur are responsible for most properties. It shows the active sites that can react with surface and affect electron transmission. Ru atom has a d electronic configuration [12] with low spin t_{2g} where S atom has S $3p$ state with up spin $PP\sigma^*$. This motivated us to confirmed that band gap depends only the position of Sulfur (parameter of structure ν) and S-S distance.

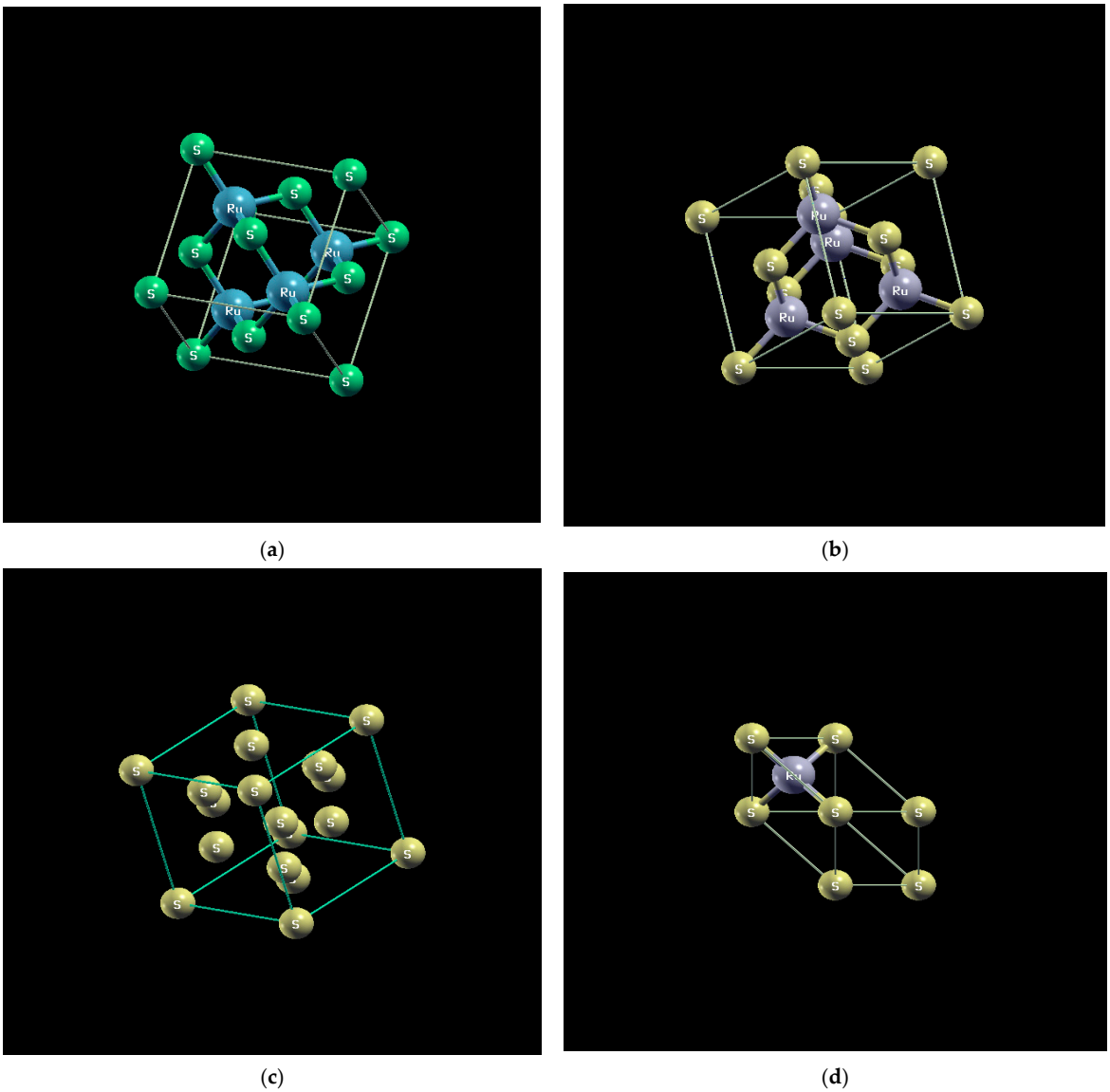

Figure 7. (**a**) crystallographic structure of Pyrite RuS_2, (**b**) crystallographic structure of pyrite RuS_2, (**c**) crystallographic structure of pyrite S_2, and (**d**) primitive cell of RuS_2.

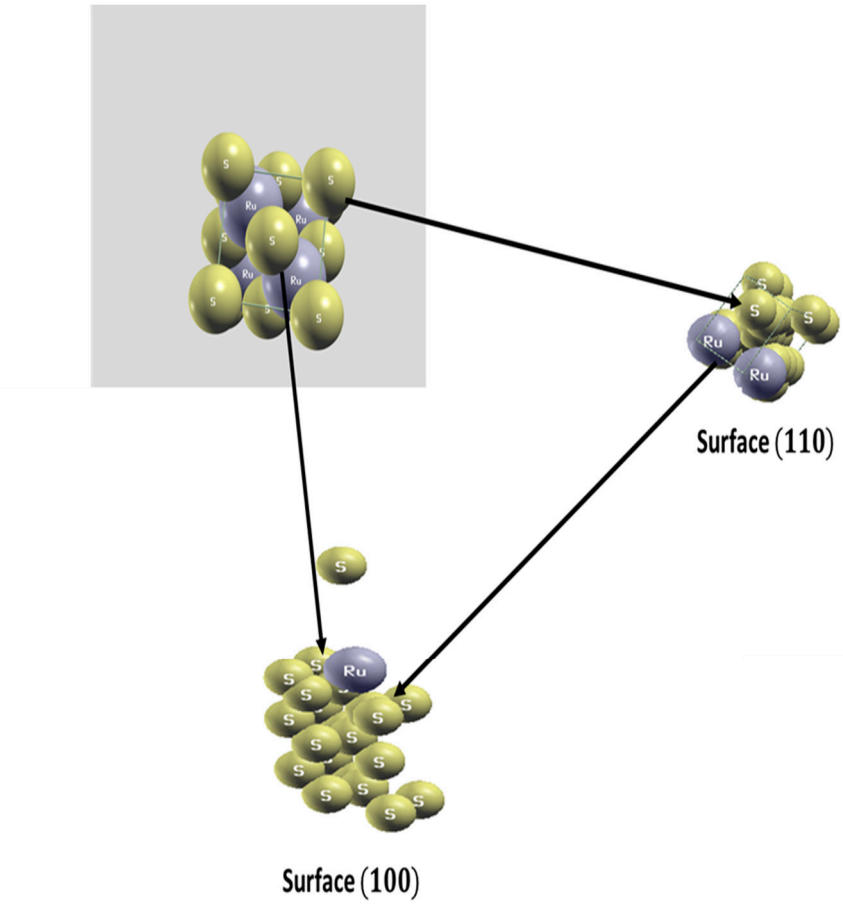

Figure 8. Distribution of sulfur in the surface (100) and the surface (110) of the pyrite RuS_2.

4. Conclusions

We have successfully prepared RuS_2 by the chemical vapor transport method. Obtaining RuS_2 at a low temperature is practically impossible [13]. We have determined the energy gap, and sulfur–sulfur distance for different samples. In conclusion, we can obtain RuS_2 at a low temperature (900 °C and 950 °C) with an important stoichiometry shift of sulfur, for samples CS9 and CS8.

Our work shows a strong dependence between the sulfur–sulfur distance and the energy gap on the temperature, which leads us to the conclusion that when the growth parameter increases, the energy gap decreases. Furthermore, our results have demonstrated that in comparison with the GaAS semiconductors in [14,15] pyrite RuS_2 has different gaps. Moreover, pyrite RuS_2 is the best candidate for multispectral solar cells.

Author Contributions: Conceptualization, R.S., O.G., H.E.; Investigation, R.S., E.A.A.; Validation, R.S., Writing (original draft), R.S., E.A.A., H.E.; Project administration, O.G., H.E.; Supervision, O.G., H.E.; Resources, O.G., H.E.; Software, E.A.A. All authors have read and agreed to the published version of the manuscript.

Funding: This research received no external funding.

Institutional Review Board Statement: Not applicable.

Informed Consent Statement: Not applicable.

Data Availability Statement: Not applicable.

Acknowledgments: We would like to thank Laboratoire de Physique du Solide au CNRS de Bellevue (LPSB) for letting us use their lab for our experimental work.

Conflicts of Interest: The authors declare no conflict of interest.

References

1. Topsoe, H.; Clausen, B.S.; Massoth, F.E. Hydrotreating Catalysis-Science and Technology. *Springer* **1996**, *14*, 1465. [CrossRef]
2. Hulliger, F. Crystal Structure and Electrical Properties of Some Cobalt-Group Chalcogenides. *Nature* **1964**, *204*, 644–646. [CrossRef]
3. Knop, O.; Reid, K.I.G.; Sutarno; Nakagawa, Y. Chalkogenides of the transition elements. VI. X-ray, neutron, and magnetic investigation of the spinels Co_3O_4, $NiCo_2O_4$, Co_3S_4, and $NiCo_2S_4$. *Can. J. Chem.* **1968**, *46*, 22. [CrossRef]
4. Harris, S.; Chianelli, R. Catalysis by transition metal sulfides: The relation between calculated electronic trends and HDS activity. *J. Catal.* **1984**, *86*, 400–412. [CrossRef]
5. Ezzouia, H.; Heindl, R.; Parsons, R.; Tributsch, H. Visible light photo-oxidation of water with single-crystal RuS_2 electrodes. *J. Electroanal. Chem. Interfacial Electrochem.* **1983**, *145*, 279–292. [CrossRef]
6. Heindl, R.; Parsons, R.; Redon, A.; Tributsch, H.; Vigneron, J. Photoelectrochemical behaviour of ruthenium disulphide electrodes in contact with aqueous electrolytes. *Surf. Sci.* **1982**, *115*, 91–103. [CrossRef]
7. Ezzaouia, H.; Heindl, R.; Loriers, J. Synthesis of ruthenium and osmium dichalcogenide single crystals. *J. Mater. Sci. Lett.* **1984**, *3*, 625–626. [CrossRef]
8. Ezzaouia, H.; Foise, J.W.; Gorochov, O. Crystal growth in tellurium fluxes and characterization of RuS_2 single crystals. *Mater. Res. Bull.* **1985**, *20*, 1353–1358. [CrossRef]
9. Fiechter, S.; Kuhne, H.-M. Crystal growth of RuX_2 (X = 5, *Se*, *Te*) by chemical vapour transport and high temperature solution growth. *J. Cryst. Growth* **1987**, *83*, 517–522. [CrossRef]
10. Hulliger, F. Electrical Properties of Pyrite-Type and Related Compounds with Zero Spin Moment. *Nature* **1963**, *200*, 1064–1065. [CrossRef]
11. Ahmed, A.T.A.; Chavan, H.S.; Jo, Y.; Cho, S.; Kim, J.; Pawar, S.M.; Gunjakar, J.L.; Inamdar, A.I.; Kim, H.; Im, H. One-step facile route to copper cobalt sulfide electrodes for supercapacitors with high-rate long-cycle life performance. *J. Alloy. Compd.* **2017**, *724*, 744–751. [CrossRef]
12. Sai, R.; Gorochov, O.; Ezzaouia, H. The study of the electronic structure of RuS_2. *Results Phys.* **2021**, *26*, 104393. [CrossRef]
13. Castillo-Villalón, P.; Ramírez, J.; Maugé, F. Structure, stability and activity of RuS_2 supported on alumina. *J. Catal.* **2008**, *260*, 65–74. [CrossRef]
14. Spirkoska, D.; Efros, A.L.; Lambrecht, W.R.L.; Cheiwchanchamnangij, T.; Fontcuberta i Morral, A.; Abstreiter, G. Valence band structure of polytypic zinc-blende/wurtzite GaAs nanowires probed by polarization-dependent photoluminescence. *Phys. Rev. B* **2012**, *85*, 045309. [CrossRef]
15. Cheiwchanchamnangij, T.; Lambrecht, W. Band structure parameters of wurtzite and zinc-blende GaAs under strain in the GW approximation. *Phys. Rev. B* **2011**, *84*, 035203. [CrossRef]